ARTICLES

Thermal Behavior of 1,1-Diamino-2,2-dinitroethylene

Xue-zhong Fan, Ji-zhen Li,* and Zi-ru Liu

Xi'an Modern Chemistry Research Institute, P. O. 18, Xi'an, Shaanxi 710065, China

Received: July 26, 2007; In Final Form: October 1, 2007

The thermal behavior of 1,1-diamino-2,2-dinitroethlene (DADNE) was followed by differential scanning calorimetry (DSC) and thermogravimetry (TG). In addition, it was further investigated by the combination techniques of in situ thermolysis cell or fast thermolysis probe with rapid-scan Fourier transform infrared spectroscopy (thermolysis/RSFT-IR and fast thermolysis/RSFT-IR) and by mass spectroscopy (MS). The results showed that there was a phase transition (β-DADNE to γ-DADNE) at the temperature of 119 °C, and that the gas products of DADNE consisted of CO_2, CO, NO_2, NO, N_2O, HCN, and HNCO, of which CO_2, NO, N_2O, and HCN present themselves in both the first and second stages of DADNE decomposition process, whereas CO, NO_2, and HNCO are only caused by the second stage, in air atmosphere. The C═C and C−NH_2 bonds of DADNE molecules are broken in the first stage of the decomposition process in open air, and one of the C−NO_2 and one of the C−NH_2 bonds of the molecules are broken in the same stage under electrospray ionization condition.

1. Introduction

1,1-Diamino-2,2-dinitroethylene (DADNE), which was first synthesized in 1998 by Latypoc et al.,[1] is known to be a new energetic material with promising properties. The sensitivity of DADNE to physical stimulations (impact, friction, heat, etc.) has been extensively studied, which support our belief that DADNE is a prime candidate as the main filler in insensitive munitions.[2−5] The decomposition mechanism of DADNE has been investigated by means of density functional theory (DFT) and ab initio calculations (MP2, MP4, G2).[6,7]

The aim of this work is to study the real-time thermal decomposition of DADNE by differential scanning calorimetry (DSC), thermogravimetry (TG), the combination technique of an in situ thermolysis cell with rapid-scan Fourier transform infrared spectroscopy (thermolysis/RSFT-IR), the combination technique of a fast thermolysis probe with rapid-scan Fourier transform infrared spectroscopy (fast thermolysis/RSFT-IR),[8,9] and mass spectrometry.

2. Experimental Section

2.1. Material. DADNE was prepared from 2-methylppyrimidine-4,6-dione and purified according to ref 10 by the Xi'an Modern Chemistry Research Institute; the purity was more than 99.7%. The structure of DADNE was characterized by elemental analysis, IR spectrometry, and nuclear magnetic resonance spectrometry shown in Scheme 1.

2.2. Apparatus and Measurement Methods. DSC measurements were carried out on a TA instrument Model DSC 910S under a static atmosphere of N_2 at the pressures of 0.1 and 1 MPa with a heating rate of 10.0 °C/min. DADNE samples

SCHEME 1: Structure of DADNE

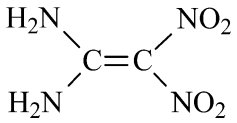

weighing from 0.5 to 1.0 mg, loaded in an aluminum sample cell, were used.

The TG measurement was made using a TGA instrument Model TA2950 under flowing N_2 gas with a heating rate of 10.0 °C/min with samples weighing from 1.0 to 2.0 mg.

Thermolysis/RSFT-IR measurements were conducted using Nicolet instrument Model NEXUS 870 FT-IR and an in situ thermolysis cell (Xiamen University, China) with the temperature range 20−455 °C anda heating rate of 10 °C/min. KBr pellet samples, well mixed by about 0.7 mg of DADNE and 150 mg of KBr, were used. Infrared spectra in the range 4000−400 cm^{-1} were acquired by a model DTGS detector at a rate of 11 files per min and 8 scans per file with 4 cm^{-1} resolution.

Fast thermolysis/RSFT-IR measurements were performed with a model 60SXR FT-IR spectrophotometer (Nicolet Instruments Co.) and an in situ thermolysis cell and a fast thermolysis probe (CDS Instruments Corporation), in the temperature range 20−600 °C with a heating rate of 50 °C/s for the linear-T/RSFT-IR test and in the temperature range 20−700 °C with a heating rate of 700 °C/s for the T-jump/RSFT-IR test. About 1.0 mg of DADNE was spread thinly on the Nichrome ribbon filament of the probe in each test. The IR spectra at 4000−600 cm^{-1} for the decomposition gas products were acquired with a model MCT-A rapid-scan IR detector, which was several millimeters above the sample surface. The experimental conditions were as follows: 5.5 files per second and 2 scans per second with a resolution of 8 cm^{-1}.

* Corresponding author. E-mail: jizhenli@126.com.

10.1021/jp075889l CCC: $37.00
Published on Web 12/01/2007

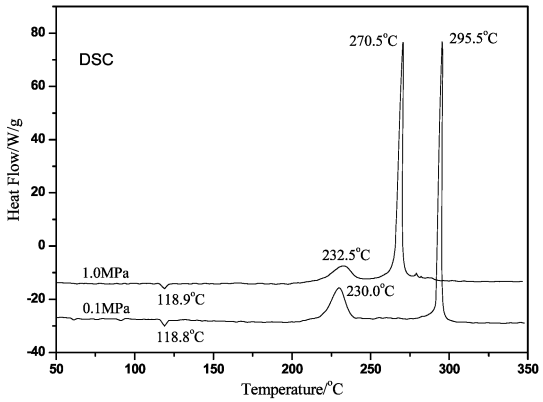

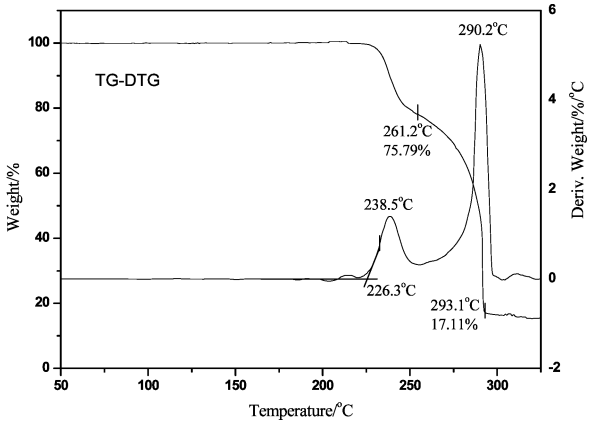

Figure 1. DSC and TG curves of DADNE.

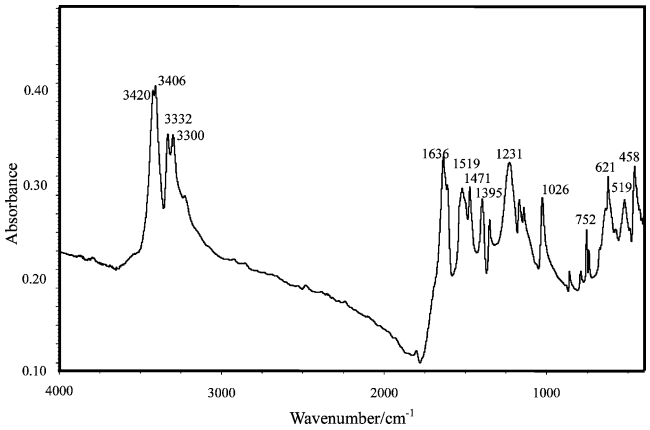

Figure 2. RSFT-IR spectrum of DADNE at room temperature.

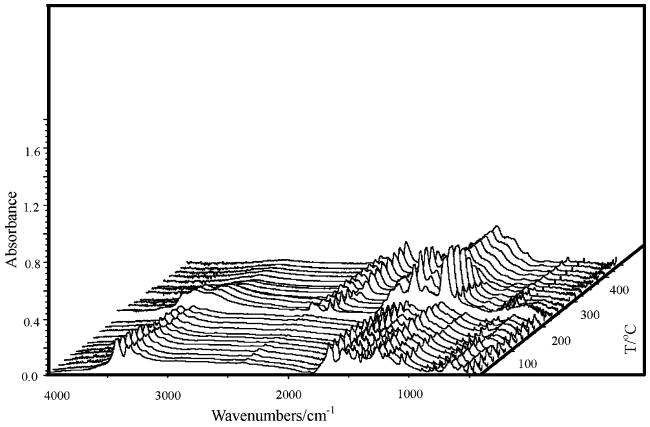

Figure 3. Overall field view of the intensity of the IR spectra of the thermal decomposition of DADNE at different temperatures in the thermolysis/RSFT-IR tests.

Mass spectra measurements were performed with a model HP5989B mass spectrograph (HP Instruments Co.) with the temperature range 150−300 °C and heating rate of 10 °C/min. The sample was inserted directly, and the temperatures of the ion source and mass analyzer were 300 and 100 °C, respectively.

3. Results and Discussion

3.1. Thermolysis on DSC and TG. The DSC and TG curves of DADNE at pressures of 0.1 and 1 MPa are shown in Figure 1.

There are one endothermic peak and two exothermic peaks in the DSC curves of DADNE at the pressures of 0.1 and 1.0 MPa, where the weak endothermic peaks at 119 °C correspond

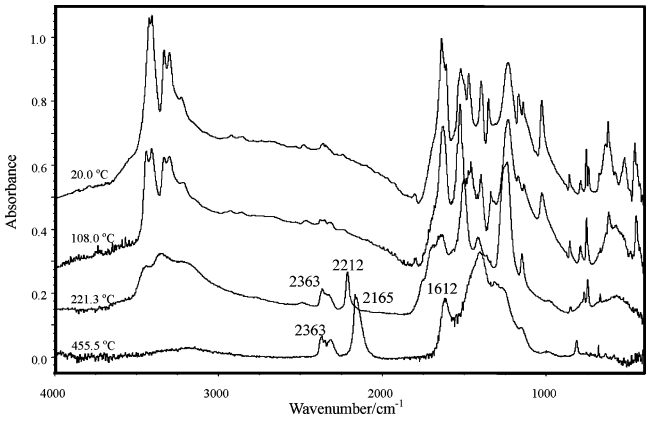

Figure 4. Typical IR spectra of the condensed products at different temperatures during the thermal decomposition process of DADNE in the thermolysis/RSFT-IR tests.

to the solid−solid phase transition of δ-DADNE to γ-DADNE,[3] and the temperature ranges of the exothermic peaks at 0.1 MPa are 216−237 and 291−297 °C, and at 1.0 MPa are 217−243 and 265−275 °C.

Two stages of mass loss processes are also shown in the TG curves. The mass loss at the first stage is 24.21%, and at the second stage is 58.68%. The final residue corresponds to the remaining carbon black (CB) due to the decomposition of DADNE.

3.2. Thermolysis in the Slowly Heated IR Cell. Thermolysis/RSFT-IR was used in real time to measure the condensed phase products of the thermal decomposition of DADNE under the linear temperature rise conditions.

The RSFT-IR spectrum of DADNE at room temperature is shown in Figure 2. The antisymmetric and symmetric stretching vibration absorptions of N−H bonds (υ_{as}(N−H) and υ_s(N−H)) at 3300, 3332 cm^{-1} and 3406, 3420 cm^{-1}, the δ(N−H) in the plane at 1636 cm^{-1} and the δ(N−H) perpendicular to the plane at 790 cm^{-1} for the N−H bonds, the υ(C−NO$_2$) at 857 cm^{-1} for the C−NO$_2$ bonds, the υ(C−NH$_2$) at 1026 cm^{-1} for the C−NH$_2$ bonds, and υ(NO$_2$) at 1395 and 1519 cm^{-1} for the N−O bonds can be observed.

The IR spectra of DADNE and the intensity of IR spectra at different temperatures are shown in Figure 3−5, respectively. It can be clearly seen that the intensity of IR spectra makes an obvious change in the temperature range 104−112 °C, where the absorption bands at 1519 and 3420 cm^{-1} move to the higher frequencies 1526 and 3440 cm^{-1}, and the absorption bands at 1636 and 1026 cm^{-1} move to lower frequencies 1627 and 1023 cm^{-1}. In the temperature range 213−221 °C, the absorp-

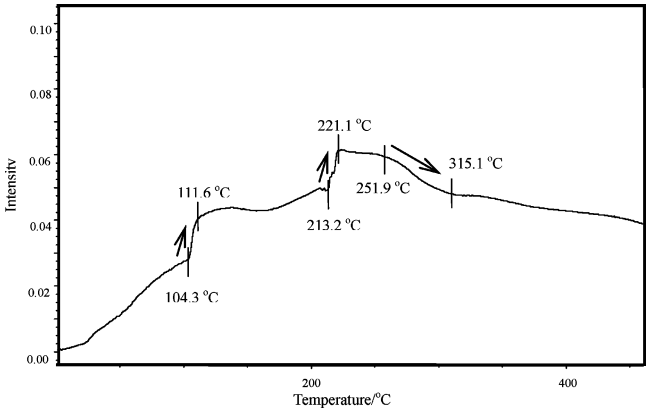

Figure 5. Intensity of IR spectra at different temperatures during the thermal decomposition process of DADNE in the thermolysis/RSFT-IR tests.

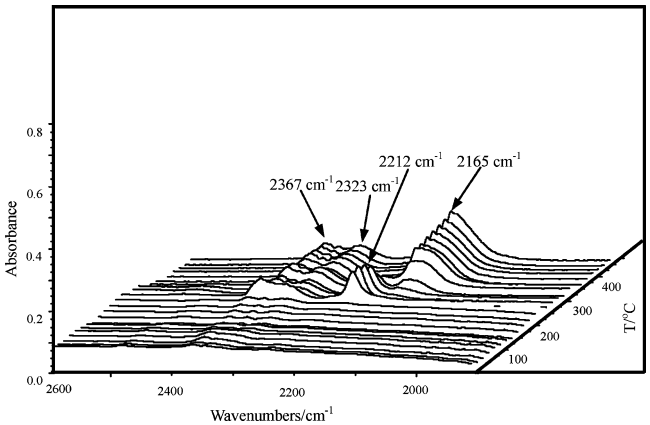

Figure 6. Close-up of the intensity of the absorption bands at 2367, 2323, 2212, and 2165 cm^{-1} of the IR spectra of thermal decomposition of DADNE at different temperatures in the thermolysis/RSFT-IR tests.

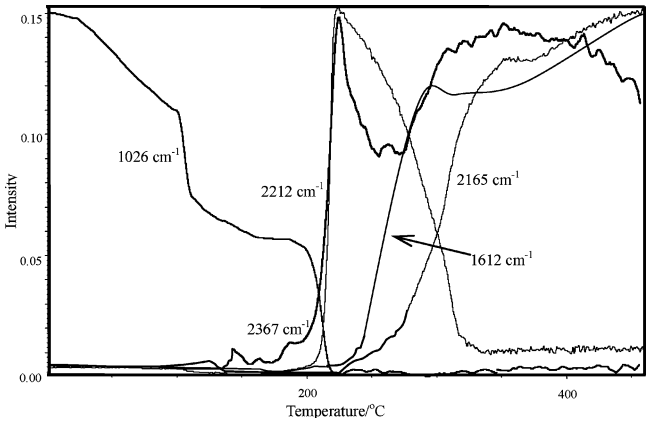

Figure 7. Intensity vs temperature curves of 2367, 2212, 2165, 1612, and 1026 cm^{-1} IR absorption peaks in the thermolysis/RSFT-IR tests.

tion bands at 3300, 3332, 3406, 3420, 1636, 1026, and 790 cm^{-1} weaken rapidly, and the bands at 2367, 2323, 2212, and 670 cm^{-1} emerge. In the temperature range 252−315 °C, the band at 2212 cm^{-1} weakens, and the bands at 2165 and 1612 cm^{-1} emerge.

The IR characteristic bands of DADNE and its decomposition products are chosen to plot the intensity vs temperature curves. Intensity vs temperature curves of the absorption bands at 2367, 2323, 2212, 2165, and 1026 cm^{-1} and their derivative curves are shown in Figures 6 and 7.

It is clear that there are two weakening steps in the intensity vs temperature curve of 1026 cm^{-1} in the temperature ranges 104−112 and 213−221 °C, which correspond to the solid−

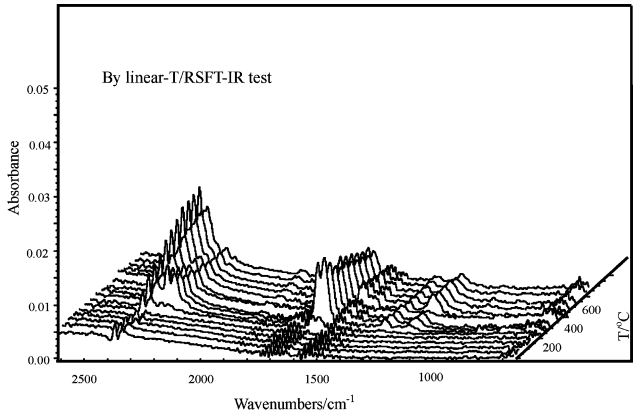

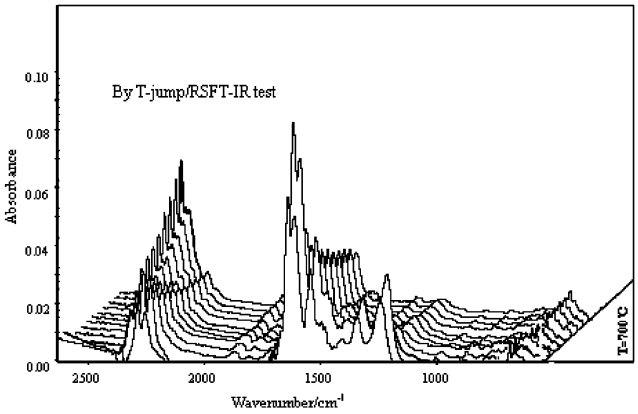

Figure 8. Typical IR spectra of the gas products at different temperatures during the thermal decomposition process of DADNE obtained by linear-T/RSFT-IR and T-jump/RSFT-IR tests.

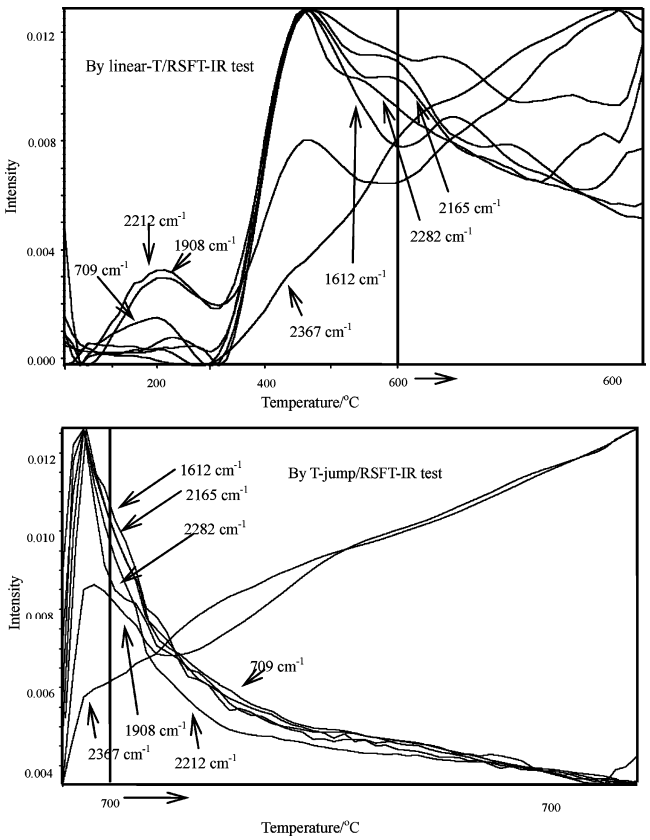

Figure 9. Intensity vs temperature curves of 2367, 2282, 2212, 2165, 1908, 1612, and 709 cm^{-1} IR absorption peaks in the fast thermolysis/RSFT-IR tests.

solid phase transition of β-DADNE to γ-DADNE and the rupture of all the C═C, C−NO_2, and C−NH_2 bonds in DADNE

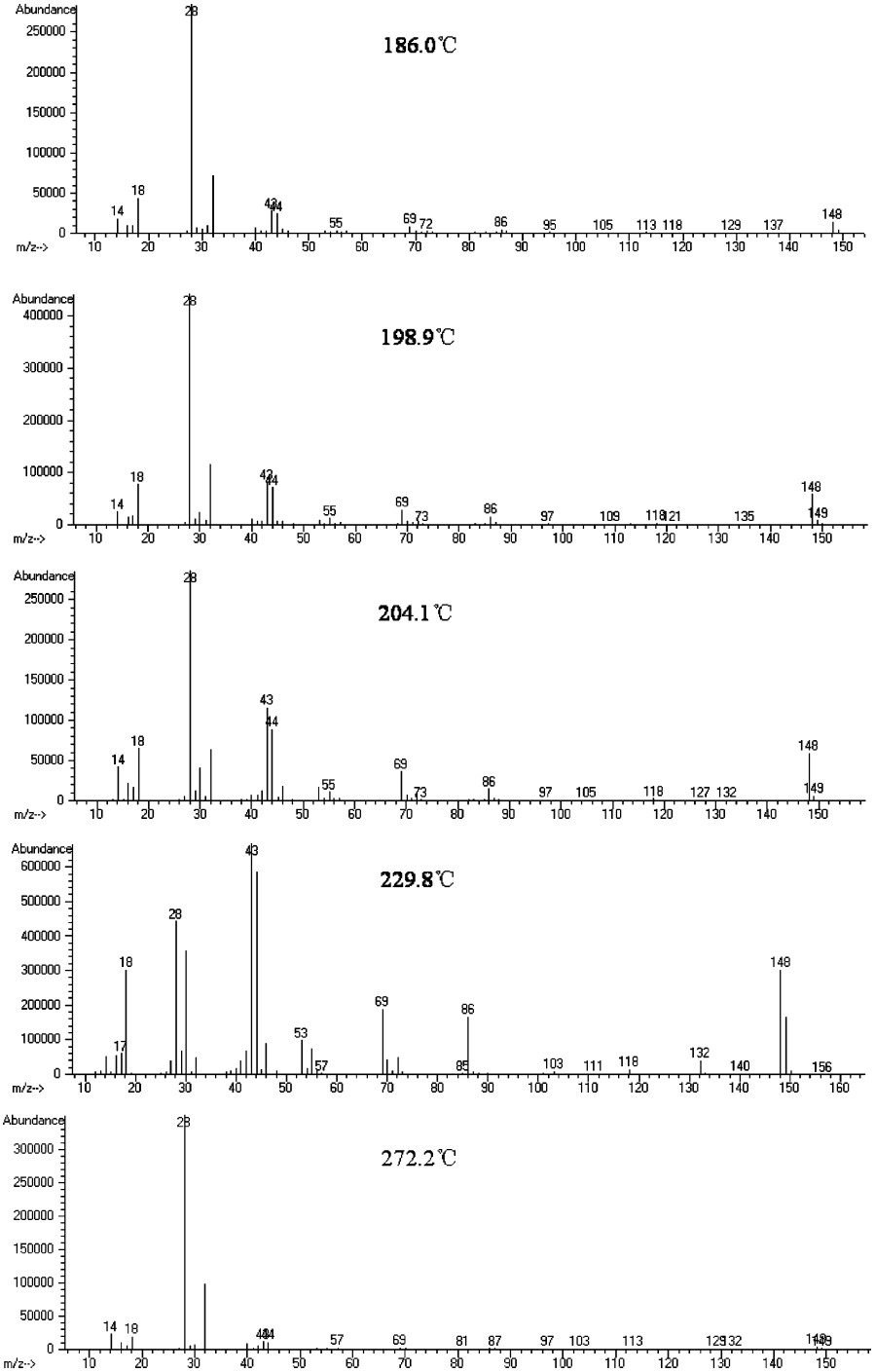

Figure 10. Mass spectra of DADNE at 186.0, 198.9, 204.1, 229.8, and 272.2 °C.

SCHEME 2: Decomposition Process of DADNE in MS

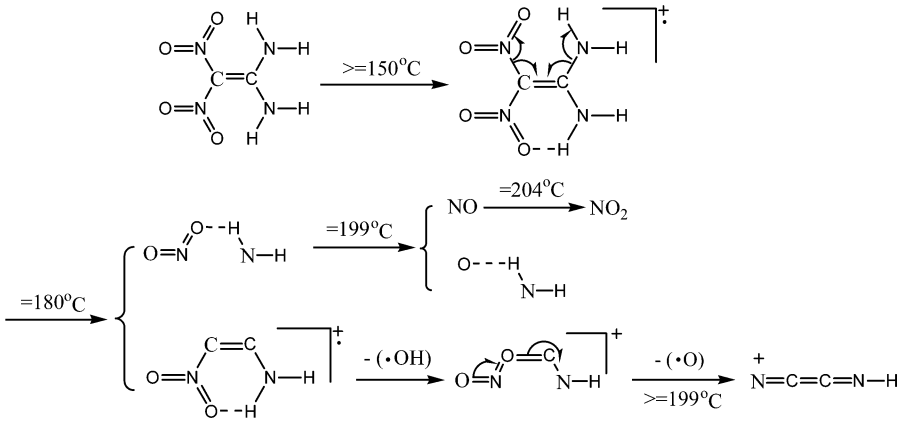

molecules, respectively. It is also obvious that the absorption peaks at 2367, 2323 cm^{-1} ($\upsilon_{as}(CO_2)$ and $\upsilon_s(CO_2)$) and at 2212 cm^{-1} ($\upsilon(N_2O)$) emerge in the temperature range 213−221 °C, the peak at 1612 cm^{-1} ($\upsilon(NO_2)$) appears in the temperature range 224−287 °C, and the peak at 2165 cm^{-1} ($\upsilon(CO)$) emerges in the range 257−336 °C. It could be concluded from the thermolysis/RSFT-IR tests that the gas products of DADNE decomposition consist of CO_2, N_2O, NO_2, and CO.

3.3. Thermolysis in the Fast Heated IR Cell. Fast thermolysis/RSFT-IR was used to measure the real-time gas products of thermal decomposition of DADNE under linear temperature rise conditions (linear-T/RSFT-IR test) and high rate temperature rise conditions (T-jump/RSFT-IR test). An overall field view and a close-up view of a few characteristic absorption bands of the intensity of IR spectra of gas products at different temperatures during the decomposition process of DADNE in linear-T/RSFT-IR and T-jump/RSFT-IR tests are shown in Figures 8 and 9, respectively.

It can be observed from Figures 7 and 8 that there are seven identified gas products in the decomposition process of DADNE. The characteristic absorption bands of CO_2, N_2O, NO, and HCN at 2367, 2212, 1908, and 709 cm^{-1} are caused by both the first and second stages of the DADNE decomposition, and the HNCO, CO, and NO_2 absorptions at 2282, 2165, and 1612 cm^{-1} are only due to the second stage of the DADNE decomposition.

3.4. Thermolysis in the Mass Spectrometry. When the sample molecules of DADNE are ionized in the source, some of the energy introduced to cause ionization serves to break up the molecule. From the illustrations of mass spectra, numerous peaks, which result from some of the molecules breaking up into fragments, lie at *m*/*z* values less than that of the molecular ion. The fragments from the breakup can help to confirm the identification and the thermal decomposition under electrospray ionization conditions of DADNE. The mass spectra of DADNE at different temperatures (186.0, 198.9, 204.1, 229.8, and 272.2 °C) are shown in Figure 10.

The *m*/*z* of 148 is found to be the DADNE molecular ion peak. From all the mass spectra of DADNE in Figure 10, it can be obviously determined that the *m*/*z* of H_2O, N_2, O_2, and CO_2 (or N_2O) at 18, 28, 32, and 44 are major relative abundance peaks throughout the test. The *m*/*z* of 86 and 69 begin to appear at about 186.0 °C, the *m*/*z* of 53 and 30 at about 199−230 °C, and the *m*/*z* of 46 at 204−230 °C.

It can be thought unassailably that the *m*/*z* of 86 is attributed to the structural formula $H_2N-C\equiv C-NO_2$ formed by the rupture of the $C-NO_2$ and $C-NH_2$ bonds of DADNE molecules. As the molecules of DADNE are impacted by the ions of different masses, the hydrogen bonds between $-N=O$ and $H-N-$ form with the temperature rise. Therefore, the formula $O=N=O\cdots H-N-H$, a neutral one, and the formula $H_2N-C\equiv C-NO_2$ appear in the ion system. That is the reason the *m*/*z* of NO_2, 46, does not appear with the $C-NO_2$ bond split at 186.0 °C, which is shown in Figure 1. NO_2 begins to appear above 204 °C.

The *m*/*z* of 69, which is attributed to the ion $(O=N-C\equiv C-N-H)^+$ formed by the loss of ·OH from the formula $H_2N-C\equiv C-NO_2$, appears simultaneously with the *m*/*z* of 86. At about 198.9 °C, ·O is split off from the formula $(O=N-C\equiv C-N-H)^+$, giving the *m*/*z* of 53 for the formula $(N=C=C-N-H)^+$.

On the basis of the above-mentioned mass spectrometry results, the decomposition steps of DADNE in MS, which are different from those in thermal analyses and thermolysis/FTIR tests and fast thermolysis/FTIR, can be expressed as in Scheme 2.

4. Conclusions

(1) The phase transition of β-DADNE to γ-DADNE is observed to take place at 119 °C, and the transition temperature is not influenced by the tested pressure.

(2) There are two stages in the decomposition process of DADNE in the temperature ranges 216−237 and 291−297 °C, the detected gas products of the first stage decomposition consist of CO_2, N_2O, NO, and HCN, and detected gas products of the second stage consist of HNCO, HCN, CO_2, CO, N_2O, NO, and NO_2.

(3) All the $C=C$, $C-NO_2$, and $C-NH_2$ bonds of DADNE molecules are broken in the first stage of the decomposition process in thermal analyses, thermolysis/FTIR, and fast thermolysis/FTIR, whereas one of the $C-NO_2$ and one of the $C-NH_2$ bonds of the molecules are broken in the first stage of DADNE decomposition in MS.

References and Notes

(1) Latypov, N. V.; Bergman, J.; Langlet, A.; Wellmar, U.; Bemm, U. *Tetrahedron* **1998**, *54*, 11525−11536.

(2) Eldsater, C.; Edvinsson, H.; Johansson, M.; Pettersson, A.; Sandberg, C. *Proc. Int. Annu. Conf. ICT, 33rd* **2002**, *63*, 1−14.

(3) Ostmark, H.; Bergman, H.; Bemm, U.; Goede, P.; Holmgren, E.; Johansson, M.; Langlet, A.; Latypov, N. V.; Pettersson, A.; Pettersson, M. L.; Wingborg, N.; Vorde, C.; Stenmark, H.; Karlsson, L.; Hihkio, M. *Proc. Int. Annu. Conf. ICT, 32nd* **2001**, *26*, 1−21.

(4) Karlsson, S.; Ostmark, H.; Eldsater, C.; Carlsson, T.; Bergman, H.; Wallin, S.; Pettersson, A. 12th Detonation (Int.) Symposium, San Diego, CA, 2002.

(5) Doll, D. W.; Hanks, J. M.; Niles, J. H. *Proceedings of the 1999 Insensitive Munitions and Energetic Materials Technology Symposium*, Tampa, FL, 1999.

(6) Glndulyte, A.; Massa, L.; Huang, L.; Karle, J. *J. Phys. Chem. A* **1999**, *103*, 11045−11051.

(7) Politzer, P.; Concha, M. C.; Grice, M. E.; Murray, J. S.; Lane, B. *J. Mol. Struct. (THEOCHEM)* **1998**, *452*, 75−83.

(8) Li, J. Z.; Zhang, G. F.; Fan, X. Z.; Hu, R. Z.; Pan, Q. *J. Anal. Appl. Pyrol.* **2006**, *76*, 1−5.

(9) Karpowicz, R. J.; Brill, T. B. *Combust. Flame* **1984**, *56*, 317−325.

(10) Holmgren, E.; Carlsson, H.; Geode, P.; Latypov, N. *Proc. Int. Annu. Conf. ICT, 34th* **2003**, *107*, 1−11.